AIAA SciTech Forum
8-12 January 2024, Orlando, FL
AIAA SCITECH 2024 Forum

10.2514/6.2024-1557

Generating maneuvering forces with oscillating propulsors

David Yudin* and Tyler Van Buren.†
University of Delaware, Newark, DE 19716, USA

Daniel Floryan‡
University of Houston, Houston, TX 77204, USA

We explore two primary ways to maneuver oscillating flexible plates in a potential flow: (1) pitch bias; and (2) asymmetric oscillating stiffness. Pitch bias will inherently provide a nonzero lift coefficient due to an average nonzero angle of attack. Alternatively, asymmetric stiffness oscillations give rise to a so-called "power stroke" which generates high positive (negative) lift during a portion of the motion, and a low negative (positive) lift during the other portion. We find that, with biased pitch the behavior followed that of thin airfoil theory superimposed onto an oscillating system for a rigid flat plate, but adding flexibility attenuated the added lift. Through oscillating flexibility, we were able to generate equal or higher average lift to the system with stiffness oscillations up to 50%. Ultimately, through combined pitch bias and asymmetric stiffness we were able to achieve a lift coefficient of $C_L = 3.6$, which exceeded the isolated pitch bias and asymmetric lift cases.

I. Nomenclature

C_L	=	coefficient of lift
C_T	=	coefficient of thrust
d	=	plate thickness
E	=	Young's modulus
h_0	=	heave amplitude
I	=	area moment of inertia
L	=	plate length
ℓ	=	dimensional lift
p	=	pressure
p_∞	=	atmospheric pressure
R	=	solid to fluid mass ratio
S	=	stiffness ratio
S_0	=	stiffness oscillation amplitude
U	=	freestream velocity
w	=	plate width
Y	=	transverse plate displacement
α	=	pitch bias
η	=	Froude efficiency
θ_0	=	maximum pitch amplitude
ρ_f	=	fluid density
ρ_s	=	solid density
μ	=	fluid dynamic viscosity
σ	=	reduced driving frequency, $\sigma = \pi f L/U$
ϕ	=	Prandtl's acceleration potential, $\phi = p_\infty - p$
ϕ_S	=	stiffness phase
$\overline{(\cdot)}$	=	(accent) time average

*Research Assistant, Department of Mechanical Engineering.
†Assistant professor, Department of Mechanical Engineering. Senior member AIAA.
‡Kalsi Assistant Professor, Department of Mechanical Engineering.

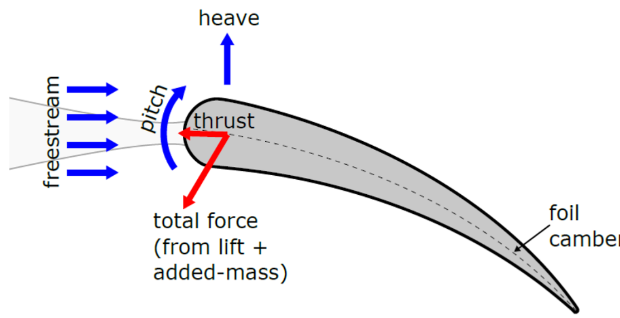

Fig. 1 Schematic of thrust from a periodically pitching and heaving flexible foil in a crossflow.

II. Introduction

Oscillating foils are consistently used by nature in both swimming and flying as a propulsion mechanism. As shown in figure 1, a forward moving foil can produce thrust force with periodic oscillation due to the foil lateral velocity. Unsteady propulsion methods are increasingly being used for propulsion of human-built uncrewed vehicles due to their their promising propulsive properties compared to traditional methods like propellers. These methods are heavily inspired by biological swimmers and fliers [1]. Through observation we know that swimmers can change their effective shape and camber while swimming, which is suggestive of active muscle usage while swimming to potentially change performance. We extend the work of [2] to study the ability of biological swimmers or fliers to generate lift as a means to maneuver while swimming or flying.

Traditionally, studies have focused on the thrust and efficiency of these types of propulsors in rectilinear swimming. However, much less attention has been given to maneuvering forces, as in producing non-zero net side force or lift. (Note here, lift is defined as being orthogonal to the the swimming direction and not necessarily the instantaneous effective velocity into the foil). Our aim is to explore two different ways to produce net lift force for the purpose of maneuvering: (1) biasing static pitch; and (2) asymmetric oscillation of flexibility. It is important to recognize that another realistic strategy to generate side force would be through asymmetric motion, however with this solution method, and the lack of nonlinearities and flow separation, asymmetric motion would not necessarily lead to non-zero side force. In future studies we are considering full Navier-Stokes solvers to compare these three strategies more applicably.

The study of biological swimmers' fluid dynamics is tied to rigid-wing flutter theory. Theodorsen [3] first modeled the forces of oscillating foils in fluid, with Garrick [4] extending this to predict thrust and power for rigid oscillating foils, highlighting the link to swimmers. Chopra and Kambe [5] later factored in three-dimensionality effects. Anderson et al. [6] used particle image velocimetry to determine thrust and power of oscillating foils and cross-referenced these findings with inviscid theory predictions. More recently, Floryan et al. [7] confirmed propulsive scaling laws for rigid two-dimensional foils undergoing heaving and pitching, further extending this to combined movements [1].

The passive flexibility of an oscillating propulsor significantly influences its propulsion efficiency. Wu [8] was among the first to consider passive flexibility analytically, which was further explored by Katz and Weihs [9, 10] when they calculated fluid–structure interactions for a flexible foil. Numerous analytical, experimental, and computational studies have since confirmed the impact of propulsor flexibility on thrust and swimming efficiency, demonstrating that flexibility often significantly boosts thrust and efficiency compared to rigid propulsors [11–17]. Floryan and Rowley [18] further studied resonance in constant-stiffness propulsors, noting its benefits for thrust and power, though not necessarily for efficiency. This was expanded upon by [19, 20], who examined the role of nonlinearity in fluid–structure systems.

Studies on propulsor flexibility beyond uniform and passive types are sparse. Floryan and Rowley [20] considered stiffness distribution and found that more stiffness towards the leading edge increased thrust but decreased efficiency. Quinn and Lauder [21] examined tunable stiffness, demonstrating that it could optimize performance parameters. Notably, only three works have considered time-varying stiffness synchronized with the kinematics. Hu et al. [22] used a model of a flexible plate behaving as a rigid propulsor with a time-varying torsional spring, enhancing both thrust and efficiency in swimming. Shi et al. [23] studied changing flexibility in nonlinear beams relevant to micro-air vehicles. Yudin et al. [2] modified the method from Moore [24] to account for time-periodic stiffness distributions.

Using lift as a means to maneuver swimming and flying vehicles has received less attention in literature. Read et al. [25] studied the effects of pitch biasing to generate a nonzero average lift coefficient over a flapping cycle of a NACA0015 airfoil, varying pitch bias over a large range. They found that increasing the bias angle increases average lift

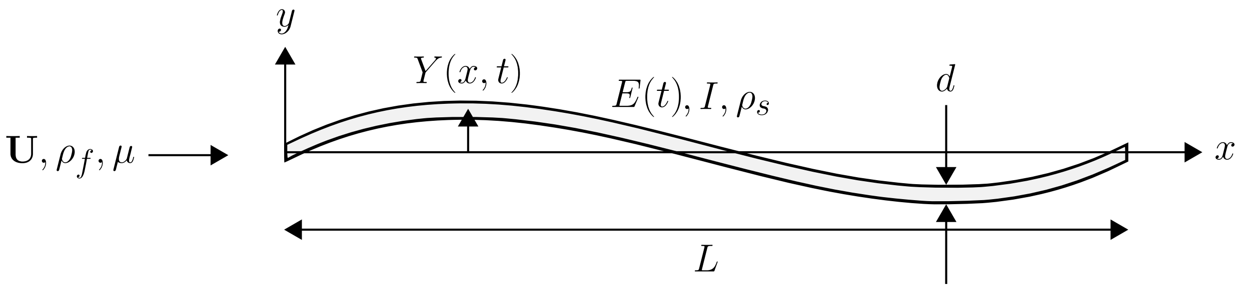

Fig. 2 A two-dimensional flat plate with time-varying Young's modulus moving through a fluid.

generation per cycle and reduces average thrust, and large drag forces can be generated which can be used for braking.

In this work, we study the effect of (1) biasing static pitch; and (2) asymmetric oscillating flexibility as means of generating nonzero lift values over a single flapping cycle. We use the semi-analytical approach described in [24], modified as in [2] in order to account for time-varying stiffness and arbitrary heaving/pitching kinematics.

While our ultimate aim is to provide a basis for maneuvering in technologies that utilize unsteady propulsion, we also aim to connect our results to the biological community. There is evidence to indicate that swimmers and fliers can change their camber during swimming or flying, respectively [26, 27]. There is no conclusion that they make use of muscle actuation on the time scale of a single flap cycle [28]. But there are studies that show that bats change the camber of their wings during flight due to the aerodynamic loads they experience [29, 30]. This could be weakly modeled by modulating the stiffness of the plate to account for the camber response of the thin membrane wing. It is possible that our simple aero- and hydrodynamic models can provide motivating evidence for biologists to look for these behaviors in animals while maneuvering.

III. Problem statement and solution methods

We consider a two-dimensional inextensible flat plate submerged in a fluid flow. We model this plate as an Euler-Bernoulli beam set in an inviscid fluid. The plate is a model for fins, wings, or propulsors of swimming and flying animals. This setup is shown in 2. Under these assumptions the system is governed by the Euler-Bernoulli beam equation and the Euler equations for the fluid flow. The Euler equations are linearized in the small-amplitude limit, for which details are given in [2]. This type of swimming is applicable to thunniform swimmers like a dolphin.

We study two cases of maneuvering, each of which is modeled using the method laid out in [2] appendix A. Pitch biasing is achieved by setting the zeroth Fourier mode of the pitching input to a nonzero value, and asymmetric stiffness is achieved by oscillating the stiffness of the plate at the same frequency as the sinusoidal heave and pitch inputs.

We nondimensionalize the equations of motion using the half-length of the plate $L/2$ as the length scale, the freestream velocity U as the velocity scale, and the convective time $L/(2U)$ as the time scale. The key nondimensional parameters are

$$R = \frac{\rho_s d}{\rho_f L}, \quad S(t) = \frac{E(t) d^3}{\rho_f U^2 L^3}, \quad \phi = p_\infty - p. \tag{1}$$

The function ϕ is Prandtl's acceleration potential [8]. The mass ratio R is the ratio of a characteristic mass of the plate to a characteristic mass of fluid, and the stiffness ratio S is the ratio of a characteristic bending force to a characteristic fluid force. The stiffness ratio, its inverse, and variations of it are sometimes called the Cauchy number [31, 32] or the elastohydrodynamical number [33].

The heave and pitch kinematics are defined as Fourier series, and can be an arbitrary periodic function

$$h(t) = \sum_{m=-\infty}^{\infty} \hat{h}_m e^{jm\sigma t}, \tag{2a}$$

$$\theta(t) = \sum_{m=-\infty}^{\infty} \hat{\theta}_m e^{jm\sigma t}. \tag{2b}$$

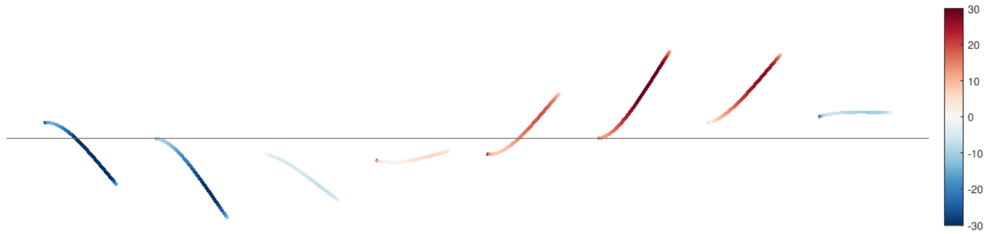

Fig. 3 Kinematics of a heaving plate actuated at its first resonant frequency of $\sigma = 3.1$. Shown is a plate with constant stiffness, color coded to represent the pressure difference across the top and bottom of the plate. Here, $\overline{S} = 20$, $h_0 = 1$, and $R = 0.01$.

For sinuisoidal heave, pitch, and stiffness, they take the form

$$h(t) = \frac{1}{2}\left(h_0 e^{j\sigma t} + h_0^* e^{-j\sigma t}\right), \tag{3a}$$

$$\theta(t) = \frac{1}{2}\left(\theta_0 e^{j\sigma t} + \theta_0^* e^{-j\sigma t}\right), \tag{3b}$$

$$S(t) = \overline{S} + \frac{\overline{S}}{2}\left(S_0 e^{2j\sigma t} + S_0^* e^{-2j\sigma t}\right), \tag{3c}$$

where $h_0, \theta_0, S_0 \in \mathbb{C}$, $j = \sqrt{-1}$, and a superscript $*$ denotes complex conjugation. The formulation in the appendices, however, is valid for generic smooth periodic functions of time. We make use of the parameter $\phi_S = \arg(S_0)$, the phase of the stiffness oscillation. Note that $|S_0|$ gives the amplitude of the stiffness oscillation as a fraction of the mean stiffness; for example, $S_0 = 0.5$ means that the stiffness oscillates with an amplitude that is 50% of the mean stiffness. For a physically meaningful (i.e., positive) stiffness, we require $|S_0| < 1$ For the plots in the paper we use $h_0 = 1$, $\theta_0 = 0$, $\bar{S} = 20$, and $R = 0.01$.

We are interested in the lift generated by the motion of the plate and the fluid flow around it. We define the coefficient of lift as

$$C_L = \int_{-1}^{1} \Delta p dx, \tag{4}$$

for small deflection angles. We relate the coefficient of lift to the dimensional lift as $C_L = \ell / \frac{1}{2}\rho_f U^2 L w$.

IV. Results

To begin, we introduce the propulsive properties of a swimming plate that can passively deform under external forces. Figure 3 shows the motion of a passively flexible plate oscillating at its leading edge. We plot a single period of motion and color code the length of the plate by the pressure difference across it. We can see during the downstroke the plate generates a high positive pressure difference on the latter half of its chord, and a high negative difference during the upstroke. In this framework, the higher the pressure difference across the plate, the higher the lift generation. In reality, it is a balance between the local slope of the plate and the pressure difference. Note that the lift generated on the upstroke is canceled out by the lift generated during the downstroke, so the net lift over one period is zero.

There are systems in both nature and industrial applications that might have active stiffness—which was studied in [2] for time-periodic stiffness. Oscillating the stiffness of the foil at the timescale of the kinematics can have a dramatic impact on the forces generated by the foil. By oscillating the stiffness S of the plate at twice the frequency of the input motions σ we achieve rectilinear swimming motion that can produce up to 35% more thrust than an equivalent plate with constant stiffness. At resonance we see a high increase in thrust from the time-periodic stiffness plate compared to the constant stiffness case. We also gain thrust before and slightly after the first resonance. In figure 4a we compare the thrust generated by a plate with constant stiffness to a plate with the same mean stiffness, but oscillating sinusoidally at twice the input frequency σ. In figure 4b We compare the efficiency of the same plates as a function of input frequency. Notice the efficiency of both plates are very similar. Near resonance the time-periodic stiffness plate is less efficient than the constant stiffness case, but only marginally. This indicates that high thrust increases can be gained with little

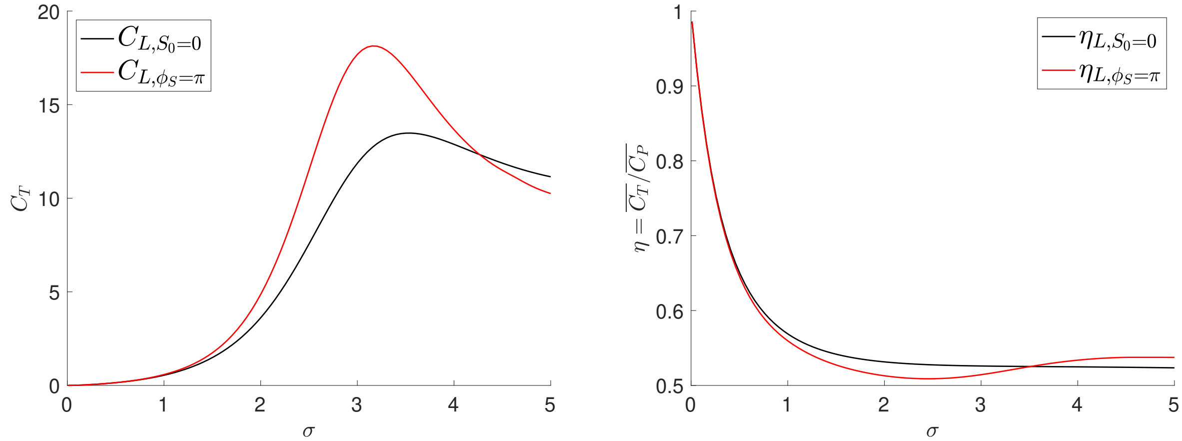

(a) **(b)**

Fig. 4 (a) Thrust coefficient as a function of reduced frequency σ for a flapping plate with constant stiffness and time-periodic stiffness. (b) Average efficiency as a function of reduced input frequency σ. For both plots $\bar{S} = 20$.

impact on efficiency. This provides the basis for using stiffness oscillation to manipulate the lateral forces produced by a periodic foil.

Now that we better understand the basic rectilinear swimming systems with zero mean side force, we consider the results of studies aimed at exploring the impact of static pitch biasing and asymmetric stiffness on maneuvering forces of an oscillating plate. In the following sections, we consider either having a statically biased pitch on the plate or asymmetric stiffness oscillation.

A. Pitch bias

Pitch bias is the most straightforward way to generate nonzero lift forces for unsteady propulsion. It gives the plate a nonzero angle of attack on average over a flapping cycle. This provides a nonzero lift force similar to quasi-steady lift-generating plates. Figure 5a shows the instantaneous lift of a plate with a pitch bias of $\alpha = 15°$. The kinematic parameters for this case are as follows: $h_0 = 1$, $\theta_0 = 0$, $\bar{S} = 20$, and $\sigma = 2.5$ The pitch bias shifts the lift curve up, causing the average lift to be nonzero. The average lift coefficients over a range of frequencies is shown in figure 5b. We see a clear resonant peak at around $\sigma = 2.3$, where the plate achieves high deflections, which in turn create large pressure differences across the plate and vice versa. Largely, across resonance of the system we see the biased pitch add a relatively constant non-zero lift coefficient for all frequencies tested.

Note that, increasing the pitch bias will increase the lift generated in one flapping cycle up to the point of the separation of the flow. Due to the assumption the flow stays attached along the entire plate we present only pitch biases where the attached flow is a reasonable assumption. We will use quasi-steady limits of angled flat plates for boundaries on our peak angles of attack.

Here we need to recognize that the above case was an heave-oscillating flexible flat plate with pitch bias. This means that the role of flexibility and unsteadiness are impacting the lift generation. In the simplest form of lift generation for a rigid flat plate, we consider steady thin airfoil theory. Here, the lift goes simply as $C_L = 2\pi\alpha$ until angles are high enough to reach separation. We can test the role that flexibility plays on this by gradually making a statically pitched plate more flexible, as shown in figure 6a. Here we see that our solution method reproduces the results of thin airfoil theory with a rigid plate, but as we reduce the stiffness of the plate we continuously lose lift generation. This makes sense, as the more flexible the plate is, the less effective camber it has, since the angle of attack is only enforced at the leading edge. We can see from figure 6b that as we approach a completely rigid plate the coefficient of lift approaches that predicted by the thin airfoil theory. As we decrease stiffness the lift decreases logarithmically between $10^0 < \bar{S} < 10^1$, and sublogarithmically outside of this range. However, for a given stiffness, the C_L verse α behavior is linear, but with a different slope than that defined by thin airfoil theory.

As a side note, we examine the effect of a rigid plate with a constant pitch angle that is also heaving up and down periodically. As it turns out the lift it generates over one cycle is simply $\overline{C_L} = 2\pi\alpha$; i.e adding unsteady motion to the

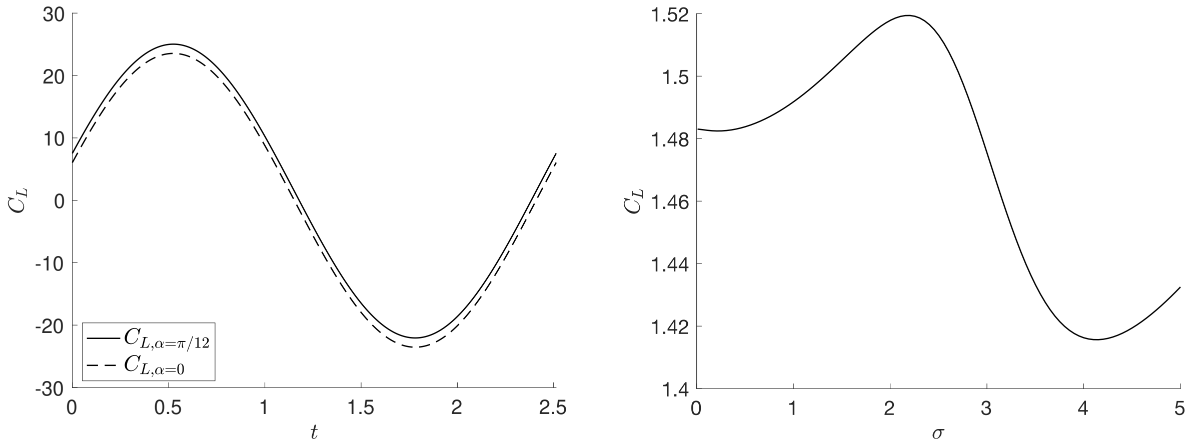

(a) **(b)**

Fig. 5 (a) Lift coefficient as a function of time for a pitched biased flapping plate with constant stiffness in time compared to a plate with no pitch bias. The equivalent plate with no pitch bias produces zero net lift. Here $\sigma = 2.5$ **The average lift over one flapping cycle is** $\overline{C_L} = 1.4871$ **(b) Average lift coefficient as a function of reduced input frequency** σ**. For both plots** $\alpha = \pi/12$**, and** $\bar{S} = 20$**.**

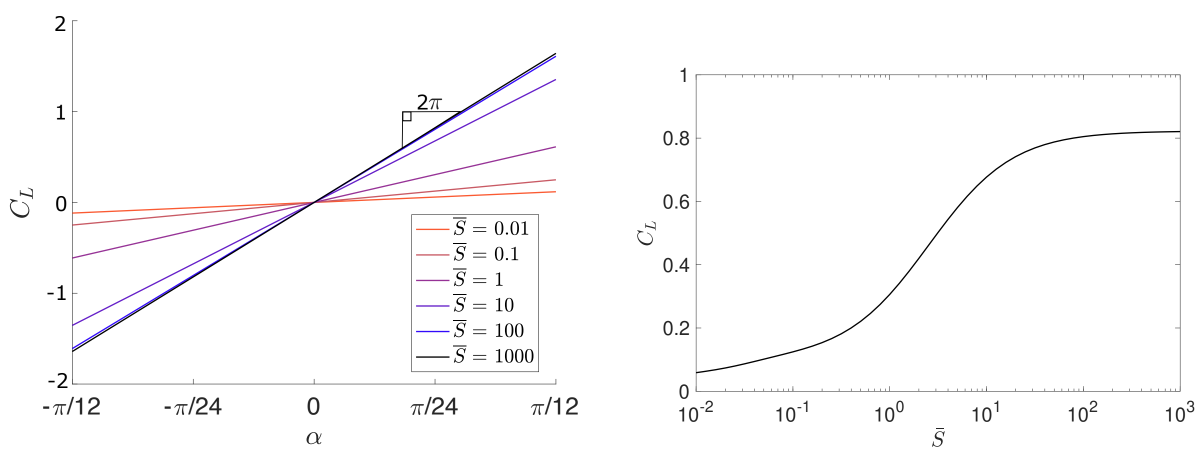

(a) **(b)**

Fig. 6 (a) Coefficient of lift as a function of the angle of attack α **as we decrease the stiffness from a rigid plate to a very flexible plate. The rigid plate follows the theory of thin airfoils:** $C_L = 2\pi\alpha$**. As we reduce the stiffness of the plate we continually reduce the lift coefficient from the ideal lift predicted by the theory. (b) Coefficient of lift as a function of the mean stiffness of the plate.**

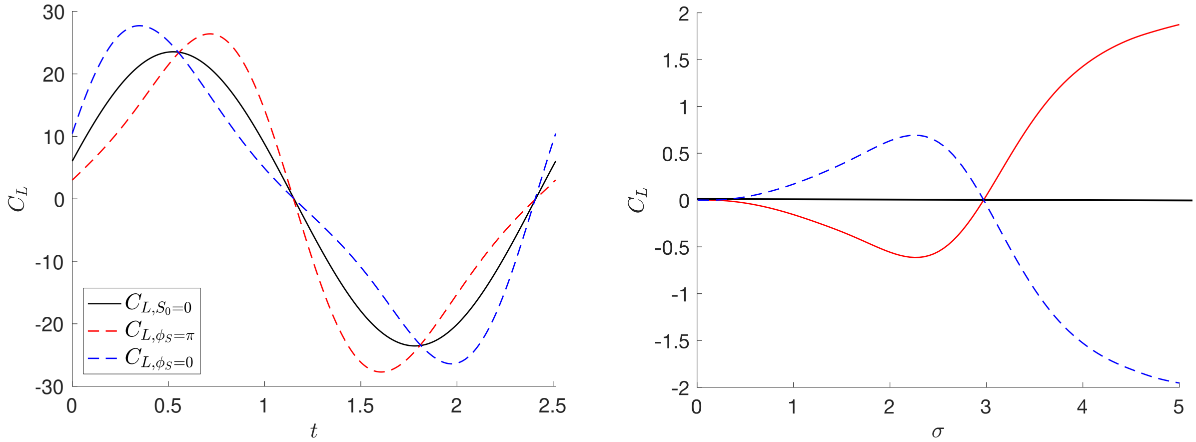

(a) **(b)**

Fig. 7 (a) Lift coefficient as a function of time for two time-periodic stiffnesses out of phase by π radians from each other. Here $\sigma = 2.5$ The average coefficient of lift for the red dashed plate is $\overline{C_L} = -0.5760$. The average coefficient of lift for the dashed blue plate is $\overline{C_L} = 0.5760$. (b) Average lift coefficient as a function of reduced input frequency σ. For both plots $\bar{S} = 20$, $h_0 = 1$, $\theta_0 = 0$ and $S_0 = 0.5$.

static angle for a rigid plate did not impact the steady thin airfoil theory results. This is not to say that unsteadiness cannot impact lift generation, as there may be added-mass consequences and attenuation to the circulation through the Theodorsen function at much higher frequencies. However, these frequencies near the first mode of resonance for a typically flexible system are representative of both biology and technology.

B. Asymmetric stiffness

Now we discuss the effect of time-varying stiffness on lift forces generated by a plate heaving with symmetric heave inputs, and with no pitch biasing. Of course, a plate with constant stiffness in this case will generate zero lift on average per cycle. By changing the stiffness of the plate with time we can essentially create a "power-stroke"; part of the flapping cycle is stiffer, which creates higher pressure forces, and in turn, lift. The other part of the cycle is less stiff and generates less lift in the opposite direction, which in turn creates a nonzero average lift over one cycle. In [2] the focus is about stiffness oscillations that are symmetric about one flapping cycle, which will generate equal and opposite lift forces on each half of the up-down motions. This is achieved by oscillating the stiffness at twice that of the input heave and pitch motion. In this paper, we oscillate the stiffness at the same frequency as the inputs, as to achieve an asymmetric up-down stiffness distribution.

Figure 7a shows the instantaneous lift of three plates: one with constant stiffness (black) and two with time-periodic stiffness (dashed blue and dashed red). The dashed blue plate oscillates its frequency in-phase with the heaving frequency σ, while the dashed red plate oscillates stiffness π radians out of phase of the heave kinematics. The average lift coefficients over a range of frequencies is shown in figure 7b. We see a clear resonant peak at around $\sigma = 2.3$, where the plate achieves high deflections, which in turn create large pressure differences across the plate and vice versa.

The average lift as a function of input frequency σ generated by the red dashed plate is the reflected function of the blue dashed plate. This is due to the stiffness phase offset of π radians; the blue red plate is stiff on the upstroke and the blue plate is stiff on the downstroke, producing opposite signed net average lift. Ultimately, asymmetric stiffness is largely capable of producing lift forces, though slightly lower in comparison to biased pitching and with much larger dependence on driving frequency.

It is clear that the timing of the stiffness oscillation is important. However, until this point, only two stiffness oscillation phases have been considered: in phase and out of phase with the kinematics. We investigate whether there is a particular phase that maximizes thrust or efficiency. In figure 8, lift is plotted on a polar plot with frequency σ on the radial axis and stiffness phase offset ϕ_s on the azimuthal axis. We see a clear peak in lift generation between $7\pi/6 < S_\phi < 4\pi/3$. But here we consider positive lift as maneuvering upwards, and negative lift as maneuvering downwards. Notice the π radian anti-symmetry; if we want to begin moving up, all we must do is rotate our stiffness

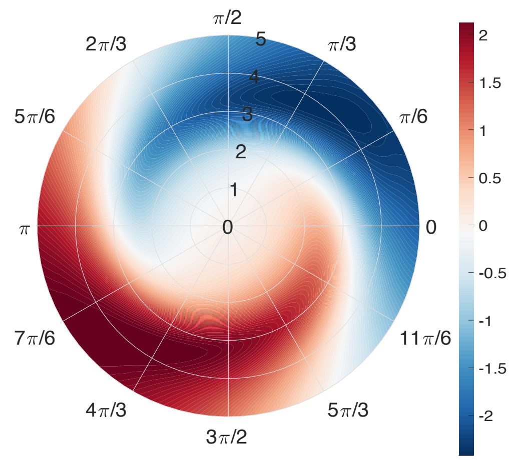

Fig. 8 Lift coefficient (color contour) as a function of driving frequency σ (radial axis) and stiffness phase S_ϕ (aximuthal axis). Here, $\overline{S} = 20$, $h_0 = 1$, $\theta_0 = 0$, and $S_0 = 0.25$.

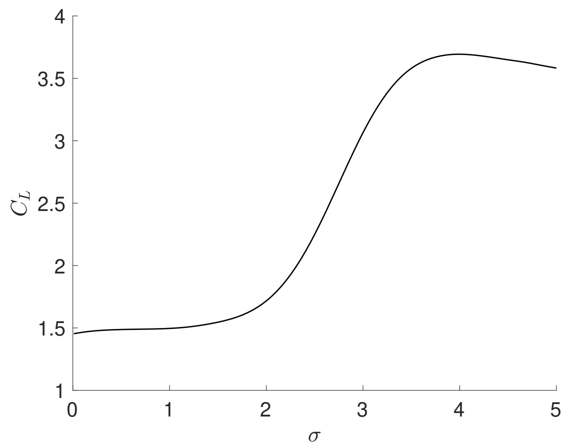

Fig. 9 Coefficient of lift as a function of driving frequency σ. Here, we use the previous analysis to pick the ideal lift generating parameters of $S_\phi = 3.9$ radians $\alpha = \pi/12$ radians, and $S_0 = 0.5$. The kinematic inputs are $h_0 = 1$, and $\theta_0 = 0.1$. The phase difference between the heave and pitch is $3\pi/2$.

phase by 180^o, which is purely a parameter and not a kinematic input.

This implies that, in a realistic swimming scenario you would choose the frequency of your propulsor to get the thrust and efficiency characteristics that you need. At this point, you could then oscillate your stiffness to generate considerable non-zero side force, and begin to maneuver. The phase of this stiffness oscillation is directly a function of the kinematic frequency in this coupled system.

C. Combined pitch bias and asymmetric stiffness oscillation

Here we compare the lift generation of the best of the last two sections: pitch bias and time-periodic stiffness to see how much of a benefit we can achieve over a rigid thin airfoil. Taking the best stiffness phase from figure 8 to be around $S_\phi = 3.9$ radians, a pitch bias $\alpha = \pi/12$ radians, and a stiffness oscillation amplitude $S_0 = 0.5$, This gives us a maximum lift coefficient, plotted in figure 9 we see a resonant peak appear at $\sigma = 3.9$, generating a peak lift coefficient $C_L = 3.6$. This shows us that even though adding flexibility to a flat plate will reduce its lift in the steady case, in the unsteady case where we can heave and pitch and change stiffness in time, the flexible plate can generate even higher lift than thin airfoil theory predicts.

V. Conclusions

In this work we introduce the concept of generating lifting forces of flexible flat plates as a simplified model for oscillating propulsors both in biological and technological systems. We show how when they are heaving and deflecting with a constant stiffness they do not generate any net lift.

The simplest method to allow these heaving and pitching plates to generate a net lift is to have a bias pitch at the leading edge. This is essentially adding an angle of attack to the plate, which would obviously generate lift. We found that this biased lift at the frequencies tested in this study followed quasi-steady thin airfoil theory, despite the addition of unsteady heaving. Flexibility did act to attenuate this lift, but the lift still behaved linearly with added pitch angle. Note that these results only apply up to the point of separation of a realistic system, and at higher frequencies we would expect a larger role of added mass forcing and lift attenuation as described by the Theodorsen function.

Additionally, we introduced the concept of asymmetric time-periodic stiffness and how it can be used to generate a nonzero lift force generation through the use of a power-stroke. Asymmetric oscillation of stiffness led to substantial lift, on the order of or even exceeding that of biasing the pitch angle. We found that the phase of this time-periodic stiffness greatly affects the lift generation, and this ideal phase was tied to the oscillation frequency and the stiffness of the plate.

Through combining the pitch bias and the asymmetric stiffness of an oscillating flexible plate, we could achieve the highest lift coefficient throughout the study of up to $C_L = 3.6$. This indicates that a flexible plate—despite attenuating the impact of the biased pitch—ultimately led to the best scenario for lift generation.

Looking forward, we hope to optimize this parameter space to find the best combination of kinematics, to explore higher frequencies and the limitations of our conclusions, and to include asymmetric kinematics through simulations and experiments that include the nonlinearities and separation characteristics in more applied systems.

Acknowledgments

Funding was supplied by the Department of Defense SMART Scholarship.

References

[1] Smits, A. J., "Undulatory and oscillatory swimming," *Journal of Fluid Mechanics*, Vol. 874, 2019. https://doi.org/10.1017/jfm.2019.284.

[2] Yudin, D., Floryan, D., and Van Buren, T., "Propulsive performance of oscillating plates with time-periodic flexibility," *Journal of Fluid Mechanics*, Vol. 959, 2023, p. A31.

[3] Theodorsen, T., "General theory of aerodynamic instability and the mechanism of flutter," *Annual Report of the National Advisory Committee for Aeronautics*, Vol. 268, 1935, p. 413.

[4] Garrick, I. E., "Propulsion of a flapping and oscillating airfoil," *Annual Report - National Advisory Committee for Aeronautics*, 1936.

[5] Chopra, M. G., and Kambe, T., "Hydromechanics of lunate-tail swimming propulsion. Part 2," *Journal of Fluid Mechanics*, Vol. 79, No. 1, 1977, p. 49–69. https://doi.org/10.1017/S0022112077000032.

[6] Anderson, J. M., Streitlien, K., Barrett, D. S., and Triantafyllou, M. S., "Oscillating foils of high propulsive efficiency," *Journal of Fluid Mechanics*, Vol. 360, 1998, p. 41–72. https://doi.org/10.1017/S0022112097008392.

[7] Floryan, D., Van Buren, T., and Smits, A. J., "Forces and energetics of intermittent swimming," *Acta Mechanica Sinica*, Vol. 33, No. 4, 2017, pp. 725–732.

[8] Wu, T. Y., "Swimming of a waving plate," *Journal of Fluid Mechanics*, Vol. 10, No. 3, 1961, p. 321–344. https://doi.org/10.1017/S0022112061000949.

[9] Katz, J., and Weihs, D., "Hydrodynamic propulsion by large amplitude oscillation of an airfoil with chordwise flexibility," *Journal of Fluid Mechanics*, Vol. 88, No. 3, 1978, p. 485–497. https://doi.org/10.1017/S0022112078002220.

[10] Katz, J., and Weihs, D., "Large amplitude unsteady motion of a flexible slender propulsor," *Journal of Fluid Mechanics*, Vol. 90, No. 4, 1979, p. 713–723. https://doi.org/10.1017/S0022112079002494.

[11] Alben, S., "Optimal flexibility of a flapping appendage in an inviscid fluid," *Journal of Fluid Mechanics*, Vol. 614, 2008, p. 355–380. https://doi.org/10.1017/S0022112008003297.

[12] Michelin, S., and Llewellyn Smith, S., "Resonance and propulsion performance of a heaving flexible wing," *Physics of Fluids*, Vol. 21, No. 7, 2009, p. 071902. https://doi.org/10.1063/1.3177356.

[13] Dewey, P. A., Boschitsch, B. M., Moored, K. W., Stone, H. A., and Smits, A. J., "Scaling laws for the thrust production of flexible pitching panels," *Journal of Fluid Mechanics*, Vol. 732, 2013, p. 29–46. https://doi.org/10.1017/jfm.2013.384.

[14] Moore, M. N. J., "Analytical results on the role of flexibility in flapping propulsion," *Journal of Fluid Mechanics*, Vol. 757, 2014, p. 599–612. https://doi.org/10.1017/jfm.2014.533.

[15] Moore, M. N. J., "Torsional spring is the optimal flexibility arrangement for thrust production of a flapping wing," *Physics of Fluids*, Vol. 27, No. 9, 2015. https://doi.org/10.1063/1.4930235.

[16] Quinn, D. B., Lauder, G. V., and Smits, A. J., "Scaling the propulsive performance of heaving flexible panels," *Journal of Fluid Mechanics*, Vol. 738, 2014, p. 250–267. https://doi.org/10.1017/jfm.2013.597.

[17] Paraz, F., Schouveiler, L., and Eloy, C., "Thrust generation by a heaving flexible foil: Resonance, nonlinearities, and optimality," *Physics of Fluids*, Vol. 28, No. 1, 2016, p. 011903. https://doi.org/10.1063/1.4939499.

[18] Floryan, D., and Rowley, C. W., "Clarifying the relationship between efficiency and resonance for flexible inertial swimmers," *Journal of Fluid Mechanics*, Vol. 853, 2018, p. 271–300. https://doi.org/10.1017/jfm.2018.581.

[19] Goza, A., Floryan, D., and Rowley, C., "Connections between resonance and nonlinearity in swimming performance of a flexible heaving plate," *Journal of Fluid Mechanics*, Vol. 888, 2020.

[20] Floryan, D., and Rowley, C. W., "Distributed flexibility in inertial swimmers," *Journal of Fluid Mechanics*, Vol. 888, 2020, p. A24. https://doi.org/10.1017/jfm.2020.49.

[21] Quinn, D., and Lauder, G., "Tunable stiffness in fish robotics: mechanisms and advantages," *Bioinspiration & Biomimetics*, Vol. 17, No. 1, 2021, p. 011002. https://doi.org/10.1088/1748-3190/ac3ca5.

[22] Hu, H., Wang, J., Wang, Y., and Dong, H., "Effects of tunable stiffness on the hydrodynamics and flow features of a passive pitching panel," *Journal of Fluids and Structures*, Vol. 100, 2021, p. 103175.

[23] Shi, G., Xiao, Q., and Zhu, Q., "Effects of time-varying flexibility on the propulsion performance of a flapping foil," *Physics of Fluids*, Vol. 32, No. 12, 2020, p. 121904. https://doi.org/10.1063/5.0027927, URL https://doi.org/10.1063/5.0027927.

[24] Moore, M. N. J., "A fast Chebyshev method for simulating flexible-wing propulsion," *Journal of Computational Physics*, Vol. 345, 2017, pp. 792–817. https://doi.org/https://doi.org/10.1016/j.jcp.2017.05.052.

[25] Read, D., Hover, F., and Triantafyllou, M., "Forces on oscillating foils for propulsion and maneuvering," *Journal of Fluids and Structures*, Vol. 17, No. 1, 2003, pp. 163–183. https://doi.org/https://doi.org/10.1016/S0889-9746(02)00115-9, URL https://www.sciencedirect.com/science/article/pii/S0889974602001159.

[26] Flammang, B. E., and Lauder, G. V., "Speed-dependent intrinsic caudal fin muscle recruitment during steady swimming in bluegill sunfish, Lepomis macrochirus," *Journal of Experimental Biology*, Vol. 211, No. 4, 2008, pp. 587–598.

[27] Adams, D. S., and Fish, F. E., "Odontocete peduncle tendons for possible control of fluke orientation and flexibility," *Journal of morphology*, Vol. 280, No. 9, 2019, pp. 1323–1331.

[28] Fish, F. E., and Lauder, G. V., Private communication, 2021.

[29] Cheney, J. A., Konow, N., Middleton, K. M., Breuer, K. S., Roberts, T. J., Giblin, E. L., and Swartz, S. M., "Membrane muscle function in the compliant wings of bats," *Bioinspiration Biomimetics*, Vol. 9, No. 2, 2014, p. 025007. https://doi.org/10.1088/1748-3182/9/2/025007, URL https://dx.doi.org/10.1088/1748-3182/9/2/025007.

[30] Swartz, S., Iriarte-Diaz, J., Riskin, D., Tian, X., Song, A., and Breuer, K., *Wing Structure and the Aerodynamic Basis of Flight in Bats*, ???? https://doi.org/10.2514/6.2007-42.

[31] Cermak, J. E., and Isyumov, N., *Wind Tunnel Studies of Buildings and Structures*, American Society of Civil Engineers, 1999. https://doi.org/10.1061/9780784403198, URL https://ascelibrary.org/doi/abs/10.1061/9780784403198.

[32] de Langre, E., "Effects of wind on plants," *Annual Review of Fluid Mechanics*, Vol. 40, 2008, pp. 141–168.

[33] Schouveiler, L., and Boudaoud, A., "The rolling up of sheets in a steady flow," *Journal of Fluid Mechanics*, Vol. 563, 2006, pp. 71–80.